Electronic Supplementary Material (ESI) for Physical Chemistry Chemical Physics.
This journal is © the Owner Societies 2019

Supporting Information

Modulation of Amyloid β Peptide Aggregation by Hydrophilic Polymers

Zhanna Evgrafova[a], Bruno Voigt[b], Andreas H. Roos[a], Gerd Hause[c], Dariush Hinderberger[a], Jochen Balbach[b] and Wolfgang H. Binder[a]*

[a] Martin-Luther University Halle-Wittenberg, Faculty of Natural Science II, Institute of Chemistry, Von-Danckelmann-Platz 4, D-06120 Halle (Saale); Germany

wolfgang.binder@chemie.uni-halle.de

[b] Martin-Luther University Halle-Wittenberg, Faculty of Natural Science II, Institute of Physics, Betty-Heimann-Str., 7, D-06120 Halle (Saale); Germany

[c] Martin-Luther University Halle-Wittenberg, Biocenter, Weinbergweg 22, D-06120 Halle (Saale); Germany

* Correspondence: wolfgang.binder@chemie.uni-halle.de; Tel.: +49 345 55 25930

Synthesis of *S*-Butyl-*S*-dodecyltrithiocarbonate (CTA-D)

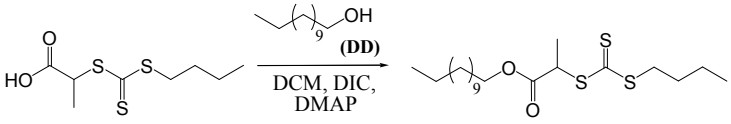

Scheme S1 Synthetic pathway for preparation of ***S*-Butyl-*S*-dodecyltrithiocarbonate (CTA-D)**

The synthesis of *S*-Butyl-*S*-dodecyltrithiocarbonate (**CTA-D**) was performed similarly to the procedure described in literature (Scheme S1)[1]. 2-{[(Butylsulfanyl)carbonothioyl]sulfanyl}propanoic acid (**CTA-C**)[2] (462.3 mg; 1.94 mmol), dodecanol (**DD**) (479.1 μL; 2.13 mmol) and 12 ml of dry and degassed DCM were added into a dry oxygen-free double-neck reaction flask equipped with a magnetic stirrer, a rubber septum and a gas tap. 4-(Dimethylamino)-pyridin (DMAP) (23.7 mg; 0.194 mmol) was added and the mixture was cooled to 0 °C by means of the ice-bath. Then, N,N′-diisopropylcarbodiimide (DIC) (330.4 μL; 2.13 mmol) solution in DCM (4 ml) was added dropwise while stirring. The reaction was hold at 0 °C for the next 2h and subsequently at room temperature overnight. Afterwards, all insoluble residues were filtered off and the crude product (**CTA-D**) was concentrated by rotary evaporation. Purification via column chromatography using chlorophorm was applied, obtaining a brownish product (R_f=0.86). The product (**CTA-D**) was dried in a high vacuum and analyzed by ^{1}H-NMR spectroscopy.

Yield: 83.7 %

Characterization data: **CTA-D:** ^{1}H-NMR (400 MHz, $CDCl_3$): δ = ppm 4.80 (q, 1H_n,-C*H*CH_3), 4.11 (m, 2H_l,-C*H*$_2$$CH_2O$), 3.35 (t, 2$H_o$, -SC*H*$_2$$CH_2$), 1.68 (m, 4$H_{c,p}$, ,-C*H*$_2$$CH_2$C*H*$_3$), 1.58 (d, 3$H_m$,-CHC*H*$_3$), 1.42 (dt, 2$H_q$, ,-C*H*$_2$$CH_3$), 1.26 (m, 16$H_{d-k}$, ,- CH_2C*H*$_2$$CH_2$), 0.93 (t, 3$H_r$, ,-$CH_2$C*H*$_3$), 0.87 (t, 3$H_a$, -$(CH_2)_{11}$C*H*$_3$)

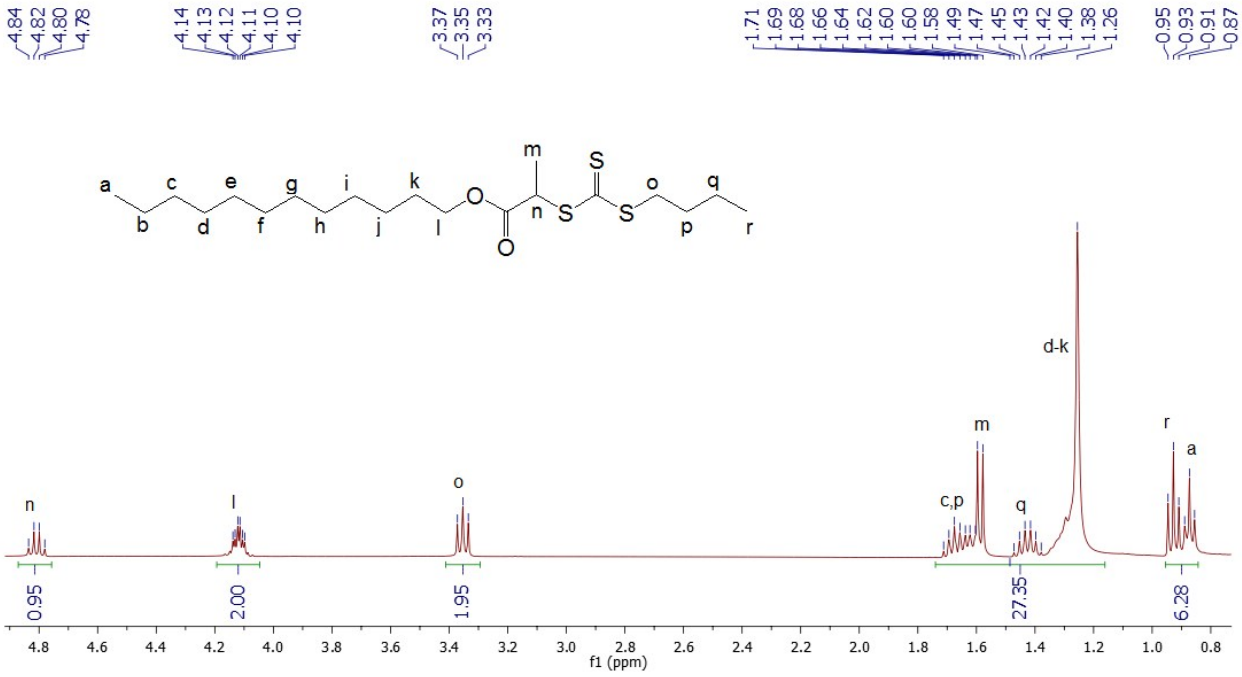

Figure S1. ^{1}H-NMR spectrum of *S*-Butyl-*S*-dodecyltrithiocarbonate (**CTA-D**).

General procedure for the syntheses of the poly(methoxydi(ethylene glycol)acrylates) on example of m2C_n16:

RAFT polymerization of **m2C_n16** was carried out using a standard Schlenk technique. The 2-{[(Butylsulfanyl)carbonothioyl]sulfanyl} propanoic acid **CTA-C**[2] (40.1 mg, 0.168 mmol), methoxydi(ethylene glycol)acrylate (**Mon-2**) (425 µL, 2.52 mmol) and 2,2'-Azobis(2-methylpropionitrile) AIBN (2.76 mg, 0.0168 mmol) in a molar ratio of (**Mon-2**):(**CTA-C**):AIBN 15:1:0.1 were dissolved in 0.85 mL of DMF. The mixture of (**Mon-2**), (**CTA-C**), AIBN and DMF were bubbled with argon for 30 minutes prior to the reaction and placed into a preheated oil bath at 70 °C. The reaction was stirred for six hours before it was cooled by means of a methanol/liquid nitrogen bath to -80 °C. The resulting yellow polymer was precipitated three times into a high excess of *n*-hexane and dried in high vacuum for three days. The polymeric product **m2C_n16** was characterized via ^{1}H-NMR (Figure S3), matrix-assisted laser desorption/ionization mass spectrometry (MALDI-TOF MS) (Figure S12), size exclusion chromatography (SEC), and turbidimetry proving its chemical structure including the end-groups.

Table S1 Summary of the synthesized polymers (Scheme 2). Molecular mass M_n of the polymers obtained via ^{1}H-NMR spectroscopy and PDI values obtained from RI signals of GPC in THF. The name of every sample comprises: m(1-9) - the number of ethylene glycol units in the side chain of the polymer; (C), (D), (B), (P) - the end group of the polymer; (n) followed by a number – the degree of polymerization. n/a: T_{cp} above 90 °C or no sufficient solubility at RT. As reference, $A\beta_{1\text{-}40}$ in the absence of polymer showed values of t_{lag} = 3.25±0.12 h and t_{char} = 3.83±0.1 h. Mean values and corresponding standard deviations (±) for t_{lag} and t_{char} obtained from three independent measurements using piecewise linear fits are given.

Entry	Name	m	End group	M_n^{NMR}, g/mol	PDI	*T*cp, °C fib.buf	*T*cp, °C water	t_{lag}, h	t_{char}, h
1	m1**C**_n12	1	carboxy- (**C**)	1560	1.19	n/a	n/a	3.88±0.75	4.3±0.75
2	m1**C**_n32	1	carboxy- (**C**)	4200	1.16	42.4	<5	22.43±1.9	24.5±1.4
3	m1**C**_n53	1	carboxy- (**C**)	9200	1.12	n/a	n/a	-	-
4	m1**D**_n17	1	dodecyl- (**D**)	1900	1.1	n/a	n/a	-	-
5	m2**C**_n4	2	carboxy- (**C**)	700	1.25	n/a	n/a	3.48±0.49	4.6±0.5
6	m2**C**_n8	2	carboxy- (**C**)	1400	1.2	n/a	n/a	3.44±0.2	4±0.13
7	m2**C**_n16	2	carboxy- (**C**)	2800	1.15	n/a	n/a	2.78±0.06	3.6±0.1
8	m2**C**_n21	2	carboxy- (**C**)	3600	1.17	n/a	n/a	2.34±0.13	3.2±0.2
9	m2**C**_n32	2	carboxy- (**C**)	5600	1.14	80.4	75	1.6±0.19	2.5±0.1
10	m2**C**_n49	2	carboxy- (**C**)	8500	1.14	78	74.7	1.23±0.05	2.3±0.1
11	m2**B**_n19	2	butyl- (**B**)	3300	1.16	60.5	68.4	2.95±0.1	4.7±0.7
12	m2**B**_n27	2	butyl- (**B**)	4700	1.12	55.2	64.9	7.5±0.11	11±0.45
13	m2**B**_n36	2	butyl- (**B**)	6300	1.12	54.1	63.8	4.72±0.89	6.6±0.9
14	m2**D**_n16	2	dodecyl- (**D**)	2800	1.1	n/a	n/a	9.18±0.73	16±1.75
15	m2**D**_n23	2	dodecyl- (**D**)	4000	1.12	43.2	51.2	20.89±0.47	29.5±0.9
16	m2**D**_n56	2	dodecyl- (**D**)	9800	1.11	45	51.9	10.53±0.45	16.9±0.9
17	m2**P**_n18	2	pyridyldisulfide- (**P**)	3200	1.16	n/a	n/a	2.0±0.17	3.8±0.63
18	m2**P**_n38	2	pyridyldisulfide- (**P**)	6600	1.19	65.2	65.6	1.51±0.12	2.1±0.11
19	m2**P**_n50	2	pyridyldisulfide- (**P**)	8700	1,15	55.8	64.1	8.52±0.33	12.3±0.46
20	m3**C**_n10	3	carboxy- (**C**)	2180	1.18	n/a	n/a	3.59±0.52	4.1±0.7
21	m3**C**_n18	3	carboxy- (**C**)	3900	1.15	n/a	n/a	2.63±0.44	3.3±0.57
22	m3**C**_n35	3	carboxy- (**C**)	7600	1.21	n/a	n/a	3.09±0.26	3.6±0.1
23	m3**C**_n38	3	carboxy- (**C**)	8300	1.17	n/a	n/a	1.64±0.12	2.4±0.1
24	m3**C**_n47	3	carboxy- (**C**)	10250	1.17	n/a	n/a	3.38±0.38	4.2±0.39
25	m3**P**_n16	3	pyridyldisulfide- (**P**)	3500	1.14	n/a	n/a	3.48±0.24	4.3±0.36
26	m3**B**_n20	3	butyl- (**B**)	4360	1.11	n/a	n/a	2.08±0.28	2.8±0.2
27	m5**C**_n13	5	carboxy- (**C**)	4000	1.12	n/a	n/a	3.15±0.82	3.2±0.9
28	m5**C**_n17	5	carboxy- (**C**)	5200	1.1	n/a	n/a	1.95±0.38	2.2±0.45
29	m5**C**_n34	5	carboxy- (**C**)	10400	1.11	n/a	n/a	1.82±0.82	3.2±0.8
30	m5**C**_n43	5	carboxy- (**C**)	14400	1.12	n/a	n/a	1.84±0.17	2.6±0.27
31	m9**C**_n10	9	carboxy- (**C**)	4800	1.12	n/a	n/a	3.27±0.34	3.9±0.9
32	m9**C**_n14	9	carboxy- (**C**)	6700	1.11	n/a	n/a	1.66±0.21	2±0.25
33	m9**C**_n24	9	carboxy- (**C**)	11500	1.1	n/a	n/a	1.5±0.27	1.9±0.31
34	m9**C**_n30	9	carboxy- (**C**)	14600	1.19	n/a	n/a	1.71±0.18	2.2±0.15
35	m9**B**_n21	9	butyl- (**B**)	10080	1.12	n/a	n/a	4.59±1.79	4.1±1.76
36	m9**P**_n15	9	pyridyldisulfide- (**P**)	7200	1.14	n/a	n/a	3.17±0.23	4.1±0.25

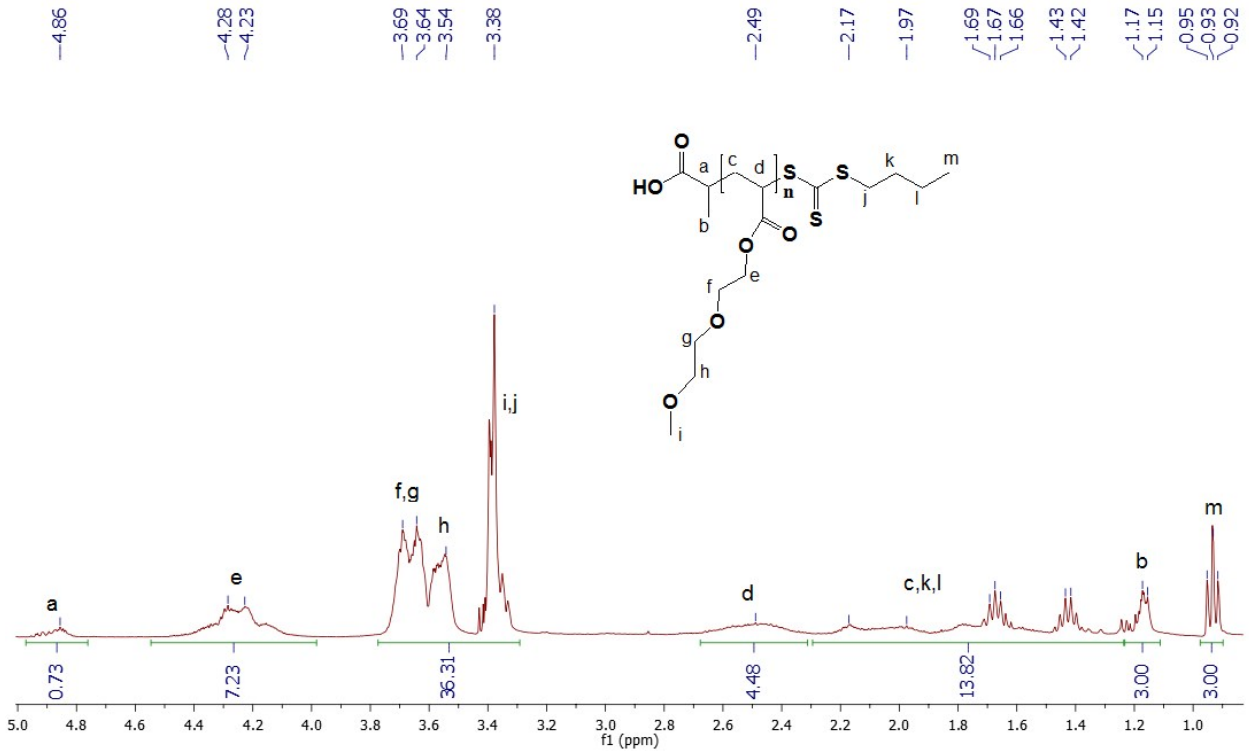

Figure S2. ^{1}H-NMR spectrum of poly(methoxy di(ethylene glycol)acrylate) (**m2C_n4**).

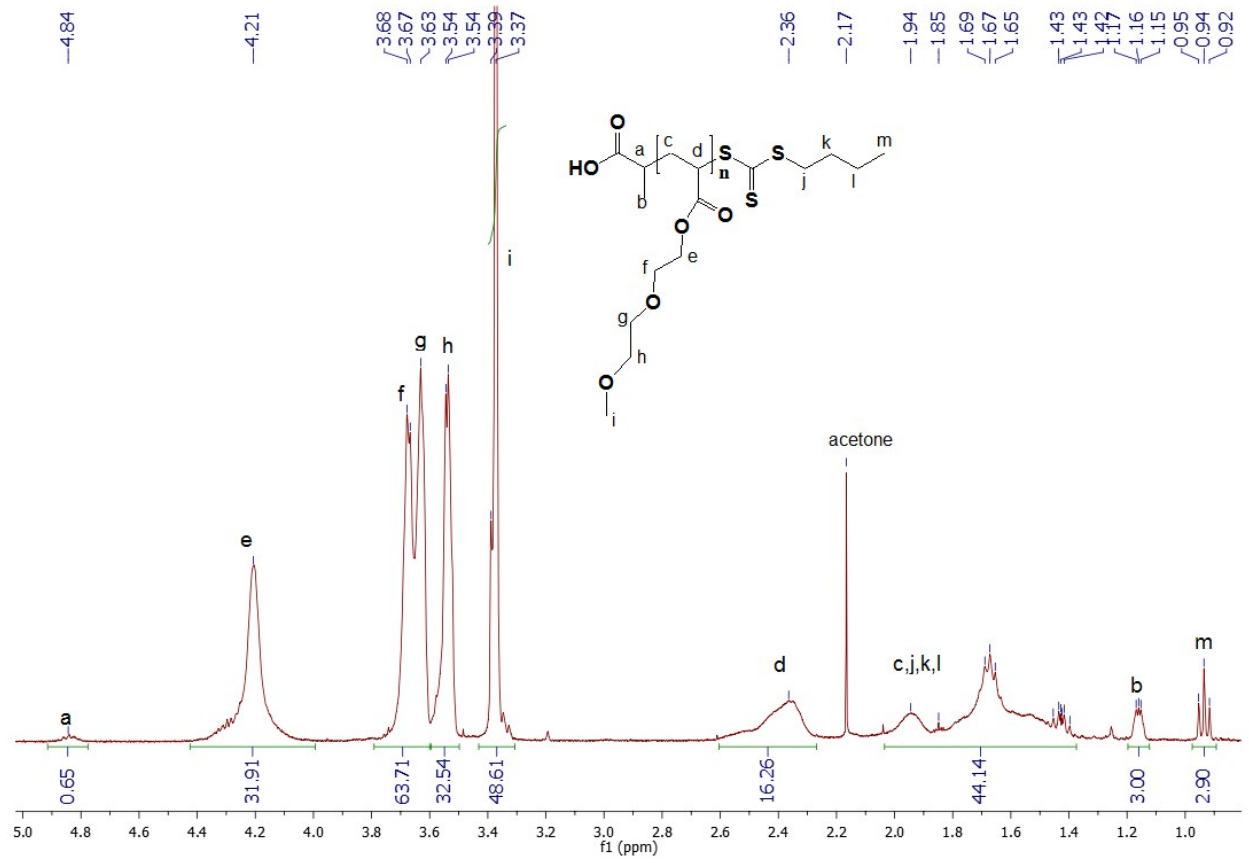

Figure S3. ^{1}H-NMR spectrum of poly(methoxy di(ethylene glycol)acrylate) (**m2C_n16**).

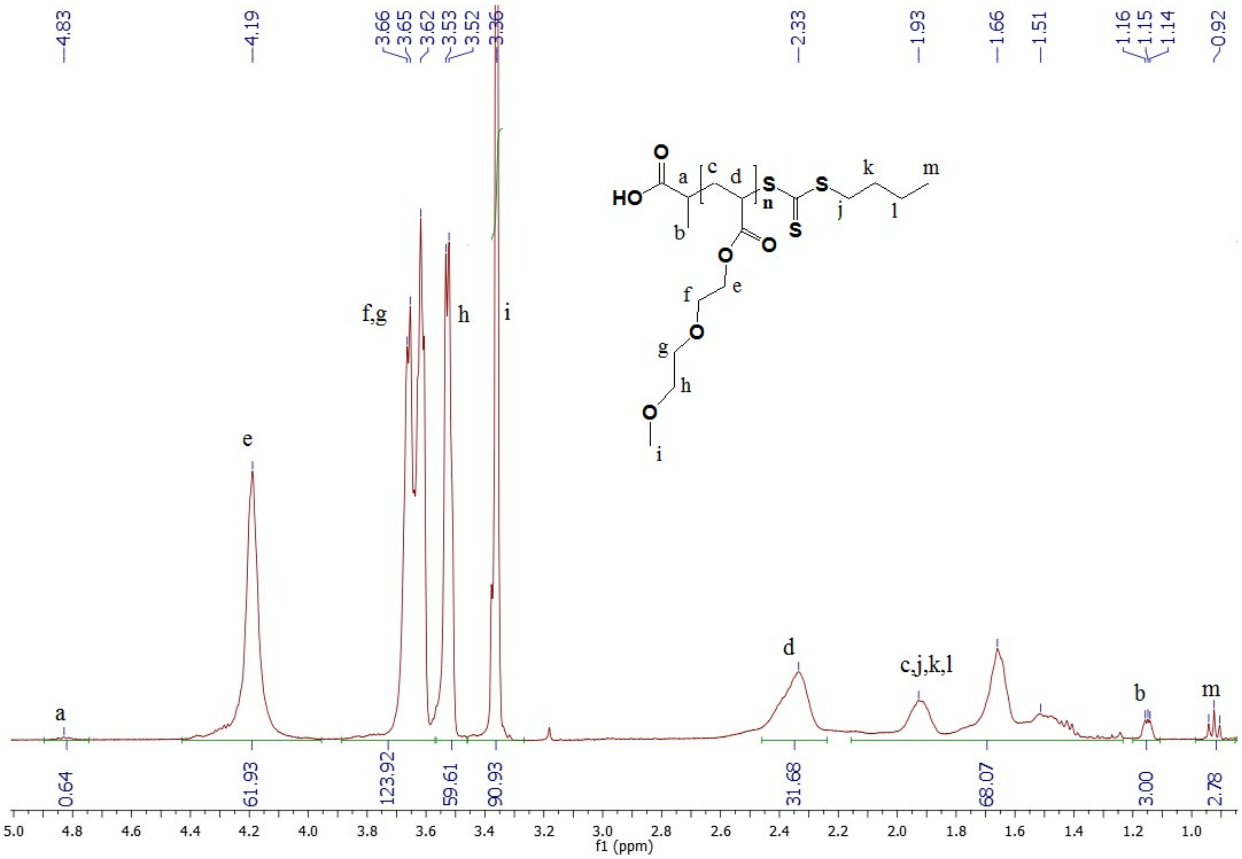

Figure S4. ^{1}H-NMR spectrum of poly(methoxy di(ethylene glycol)acrylate) (**m2C_n32**).

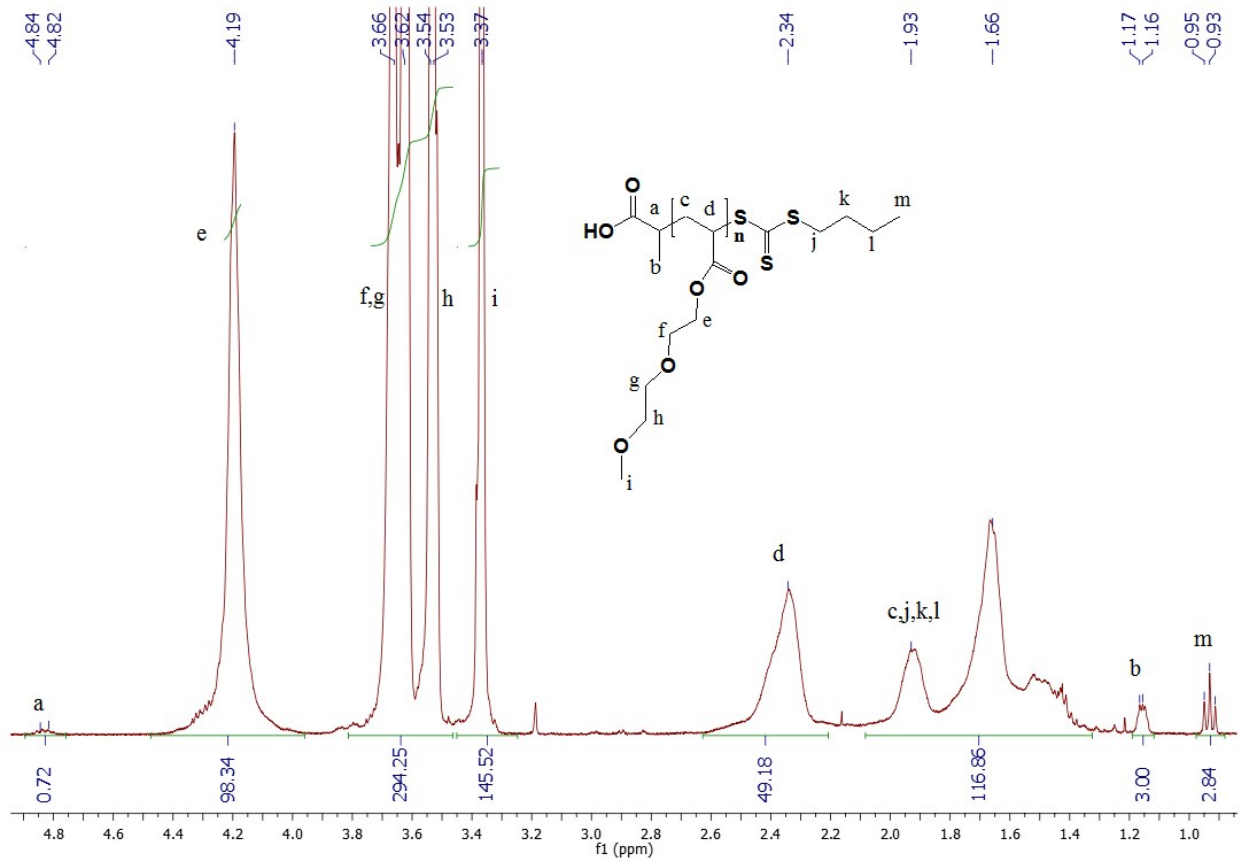

Figure S5. ^{1}H-NMR spectrum of poly(methoxy di(ethylene glycol)acrylate) (**m2C_n49**).

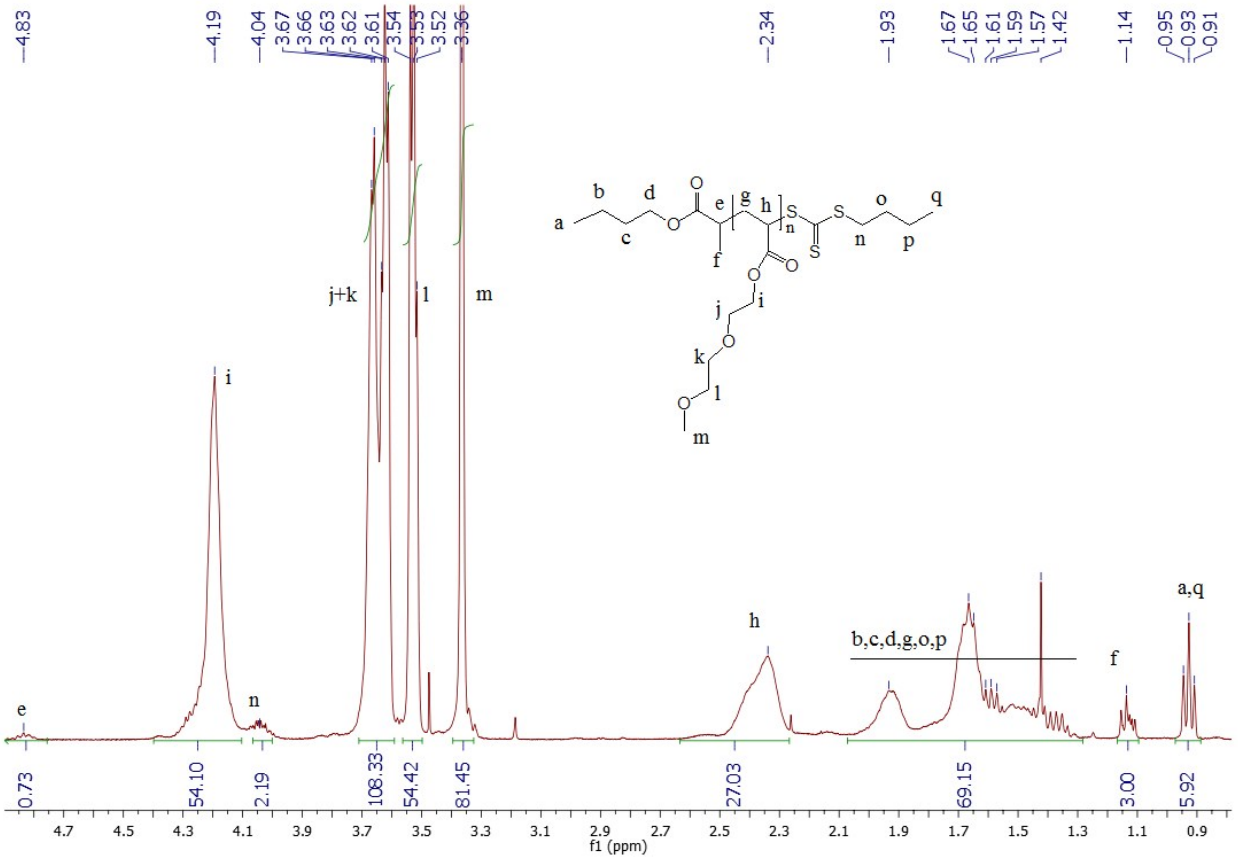

Figure S6. ^{1}H-NMR spectrum of poly(methoxy di(ethylene glycol)acrylate) (**m2B_n27**).

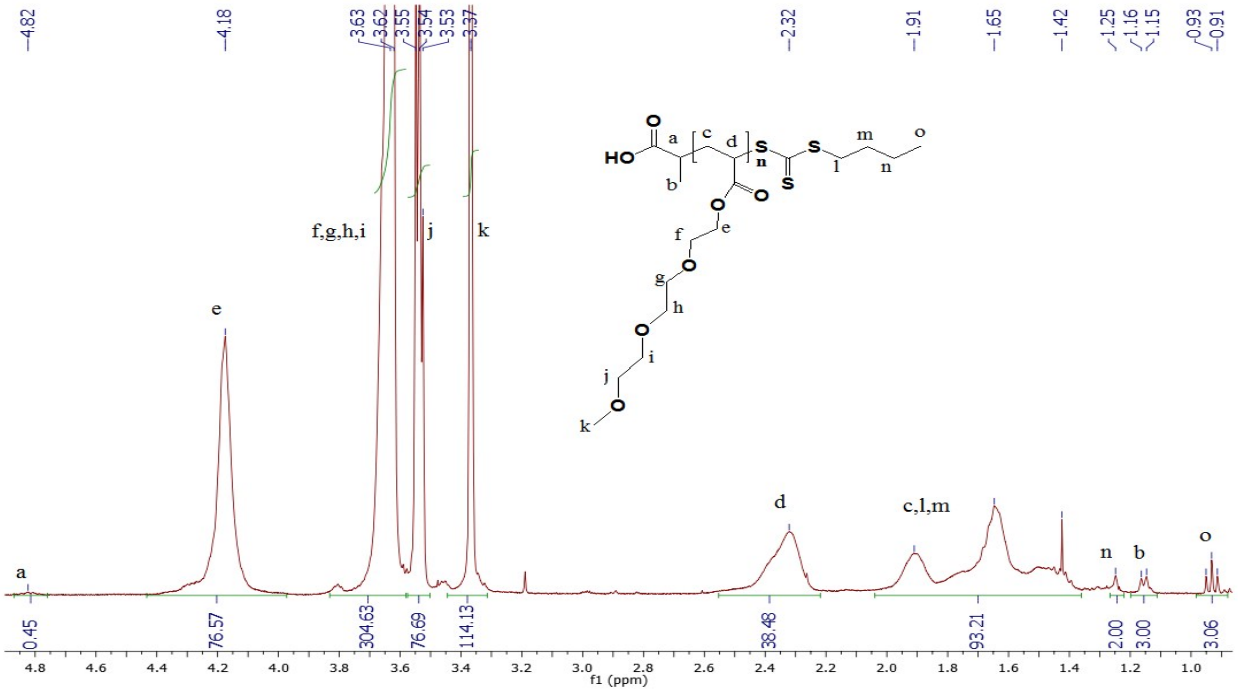

Figure S7. ^{1}H-NMR spectrum of poly(methoxy tri(ethylene glycol)acrylate) (**m3C_n38**).

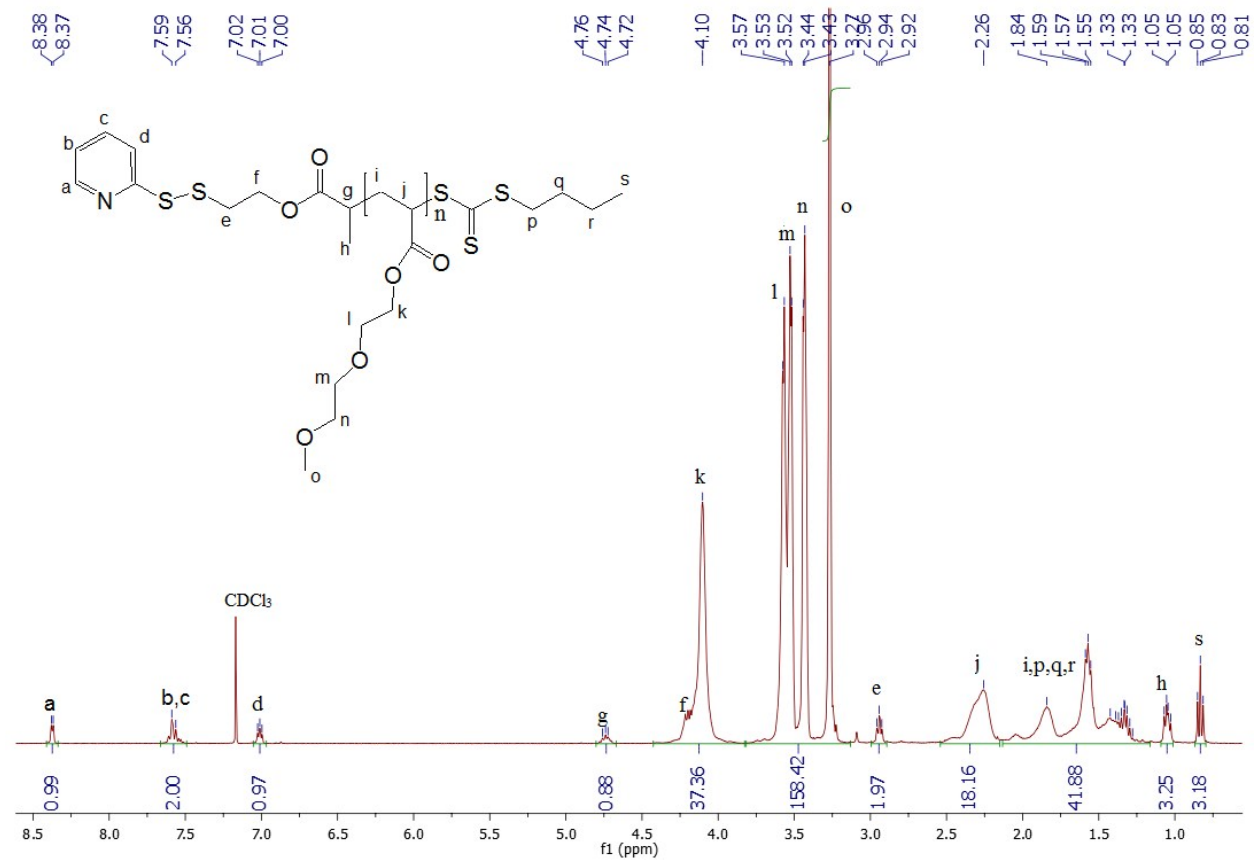

Figure S8. ^{1}H-NMR spectrum of poly(methoxy di(ethylene glycol)acrylate) (**m2P_n18**).

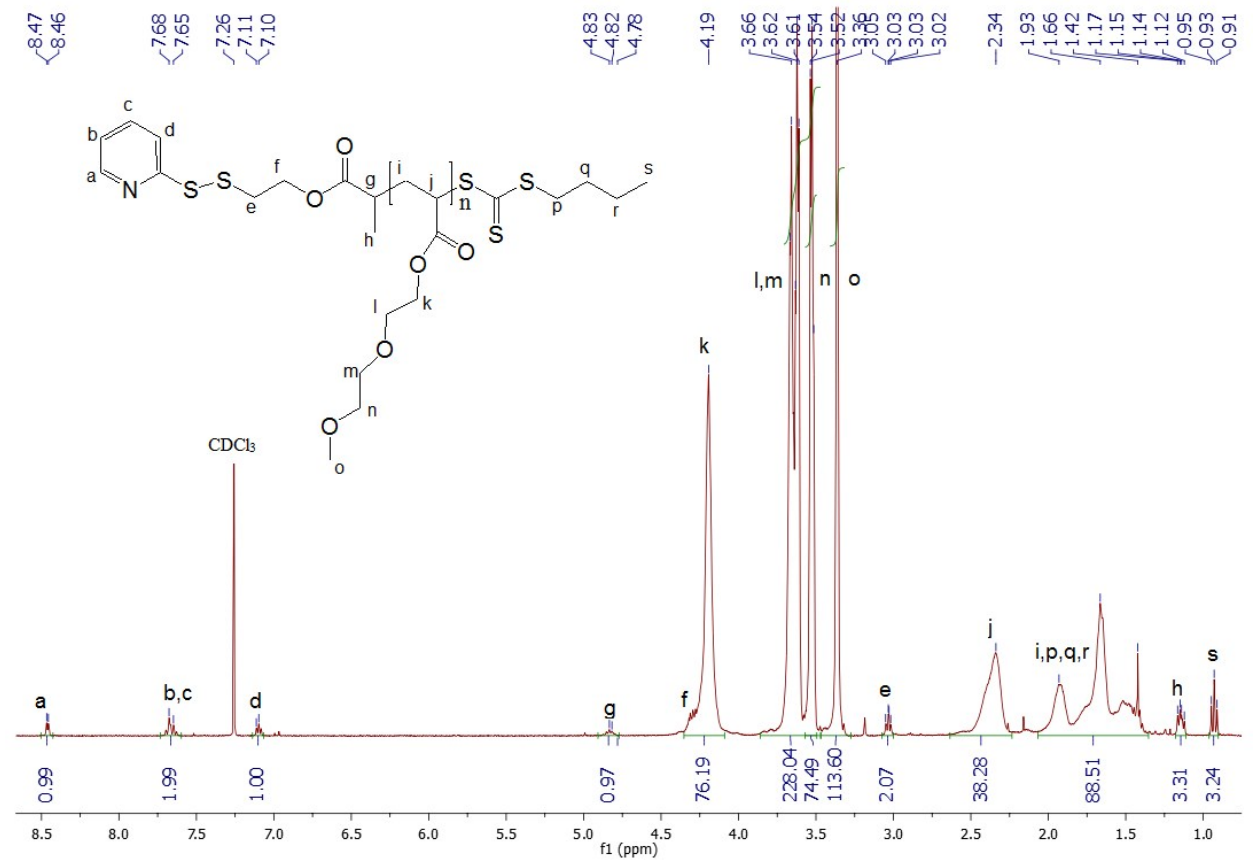

Figure S9. ^{1}H-NMR spectrum of poly(methoxy di(ethylene glycol)acrylate) (**m2P_n38**).

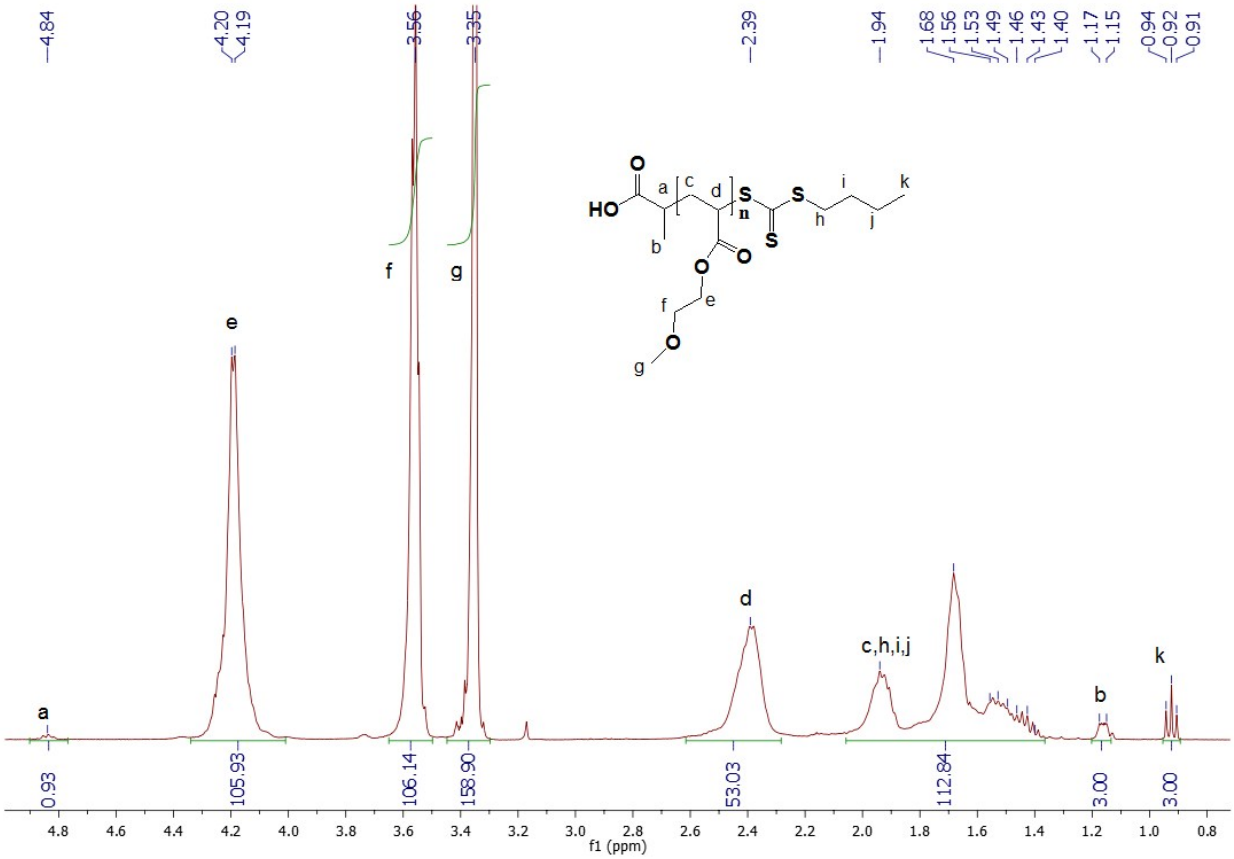

Figure S10. ^{1}H-NMR spectrum of poly(methoxy (ethylene glycol)acrylate) (**m1C_n53**).

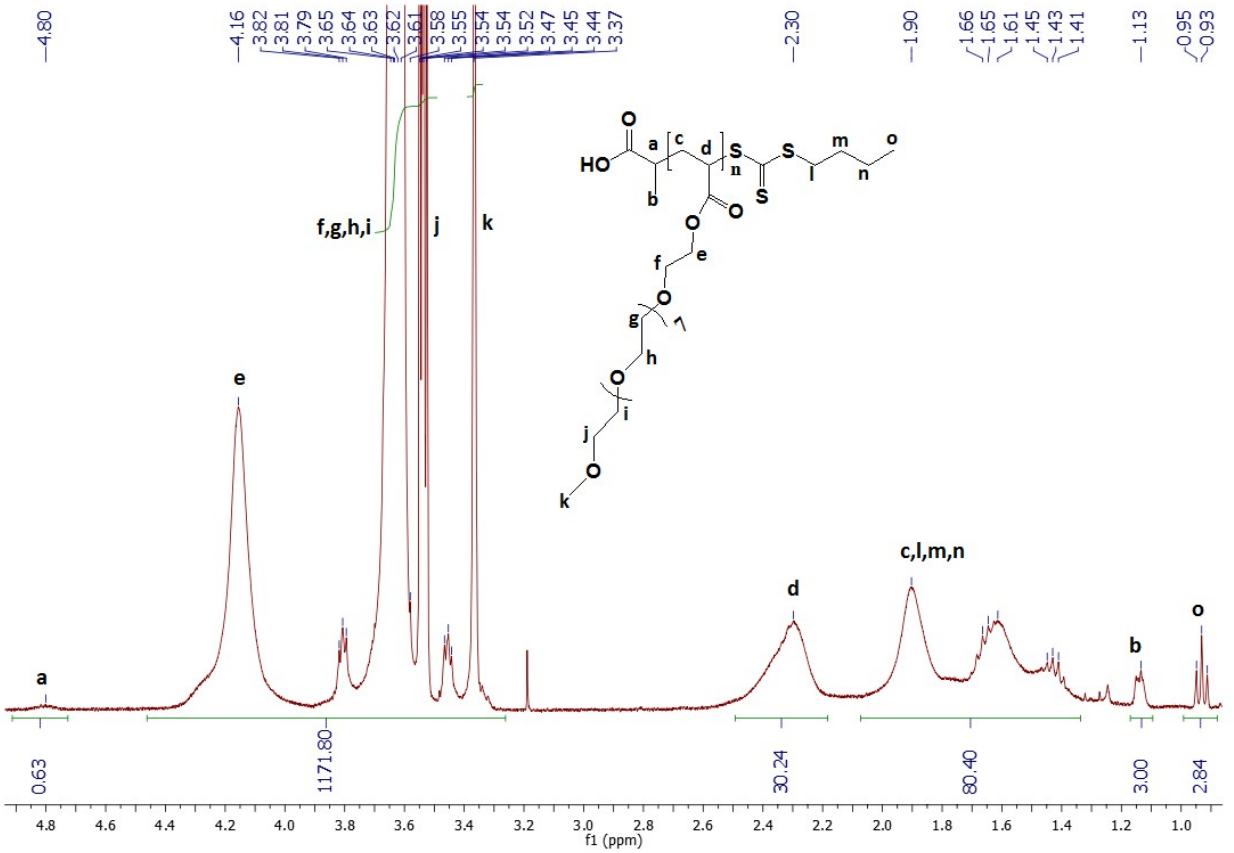

Figure S11. ^{1}H-NMR spectrum of poly(methoxy nona(ethylene glycol)acrylate) (**m9C_n30**).

m2C_n4: ^{1}H-NMR (400 MHz, $CDCl_3$): δ = ppm 4.86 (m, 1H$_a$, -C*H*CH$_3$), 4.21 (bm, 8H$_e$, -OC*H*$_2$CH$_2$), 3.64 (bm, 16H$_{f,g}$,

-OCH$_2$C*H*$_2$OC*H*$_2$), 3.54 (m, 8H$_h$, -C*H*$_2$OCH$_3$), 3.38 (m, 13H$_{i,j}$, -CH$_2$OC*H*$_3$; -SC*H*$_2$), 2.49 (bs, 4H$_d$, -C*H*CH$_2$), 1.67 (m, 12H$_{c,k,l}$, -CHC*H*$_2$; -SCH$_2$C*H*$_2$C*H*$_2$; H$_2$O from CDCl$_3$), 1.17 (m, 3H$_b$, - CHC*H*$_3$), 0.93 (t, 3H$_m$, -CH$_2$C*H*$_3$)

m2C_n8: ^{1}H-NMR (400 MHz, CDCl$_3$): δ = ppm 4.84 (m, 1H$_a$, -C*H*CH$_3$), 4.21 (bm, 16H$_e$, -OC*H*$_2$CH$_2$), 3.63 (bm, 32H$_{f,g}$, -OCH$_2$C*H*$_2$OC*H*$_2$), 3.53 (m, 16H$_h$, -C*H*$_2$OCH$_3$), 3.37 (m, 26H$_{i,j}$, -CH$_2$OC*H*$_3$; -SC*H*$_2$), 2.43 (bs, 8H$_d$, -C*H*CH$_2$), 1.67 (m, 20H$_{c,k,l}$, -CHC*H*$_2$; -SCH$_2$C*H*$_2$C*H*$_2$), 1.16 (m, 3H$_b$, - CHC*H*$_3$), 0.93 (t, 3H$_m$, -CH$_2$C*H*$_3$)

m2C_n16: ^{1}H-NMR (400 MHz, CDCl$_3$): δ = ppm 4.84 (m, 1H$_a$, -C*H*CH$_3$), 4.21 (bm, 32H$_e$, -OC*H*$_2$CH$_2$), 3.63 (bm, 64H$_{f,g}$, -OCH$_2$C*H*$_2$OC*H*$_2$), 3.54 (m, 32H$_h$, -C*H*$_2$OCH$_3$), 3.37 (m, 48H$_i$, -CH$_2$OC*H*$_3$), 2.36 (bs, 16H$_d$, -C*H*CH$_2$), 1.67 (m, 38H$_{c,j,k,l}$, -CHC*H*$_2$; -SC*H*$_2$C*H*$_2$C*H*$_2$; H$_2$O from CDCl$_3$), 1.16 (m, 3H$_b$, -CHC*H*$_3$), 0.94 (t, 3H$_m$, - CH$_2$C*H*$_3$)

m2C_n32: ^{1}H-NMR (400 MHz, CDCl$_3$): δ = ppm 4.83 (m, 1H$_a$, -C*H*CH$_3$), 4.19 (bm, 62H$_e$, -OC*H*$_2$CH$_2$), 3.62 (bm, 124H$_{f,g}$, -OCH$_2$C*H*$_2$OC*H*$_2$), 3.52 (m, 62H$_h$, -C*H*$_2$OCH$_3$), 3.36 (m, 93H$_i$, -CH$_2$OC*H*$_3$), 2.33 (bs, 31H$_d$, -C*H*CH$_2$), 1.66 (m, 68H$_{c,j,k,l}$, -CHC*H*$_2$; -SC*H*$_2$C*H*$_2$C*H*$_2$), 1.15 (m, 3H$_b$, -CHC*H*$_3$), 0.92 (t, 3H$_m$, - CH$_2$C*H*$_3$)

m2C_n49: ^{1}H-NMR (400 MHz, CDCl$_3$): δ = ppm 4.84 (m, 1H$_a$, -C*H*CH$_3$), 4.19 (bm, 98H$_e$, -OC*H*$_2$CH$_2$), 3.62 (bm, 196H$_{f,g}$, -OCH$_2$C*H*$_2$OC*H*$_2$), 3.53 (m, 98H$_h$, -C*H*$_2$OCH$_3$), 3.37 (m, 147H$_i$, -CH$_2$OC*H*$_3$), 2.34 (bs, 49H$_d$, -C*H*CH$_2$), 1.66 (m, 38H$_{c,j,k,l}$, -CHC*H*$_2$; -SC*H*$_2$C*H*$_2$C*H*$_2$; H$_2$O from CDCl$_3$), 1.16 (m, 3H$_b$, -CHC*H*$_3$), 0.93 (t, 3H$_m$, - CH$_2$C*H*$_3$)

m2B_n27: ^{1}H-NMR (400 MHz, CDCl$_3$): δ = ppm 4.83 (m, 1H$_e$, -C*H*CH$_3$), 4.19 (bs, 54H$_i$, –OC*H*$_2$CH$_2$), 4.19 (m, 2H$_n$, -SC*H*$_2$), 3.62 (bm, 108H$_{j,k}$, –OCH$_2$C*H*$_2$OC*H*$_2$), 3.53 (m, 54H$_l$, - C*H*$_2$OCH$_3$), 3.36 (s, 81H$_m$, - CH$_2$OC*H*$_3$), 2.34 (bs, 27H$_h$, - CH$_2$C*H*), 1.67 (m, 64H$_{b,c,d,g,o,p}$, -OC*H*$_2$C*H*$_2$C*H*$_2$CH$_3$; -C*H*$_2$CH; -SCH$_2$C*H*$_2$C*H*$_2$; -C*H*$_2$CH$_3$; H$_2$O from CDCl$_3$), 1.14 (m, 3H$_f$, - CHC*H*$_3$), 0.93 (t, 6H$_{a,q}$, - CH$_2$C*H*$_3$)

m3C_n38: ^{1}H-NMR (400 MHz, CDCl$_3$): δ = ppm 4.82 (m, 1H$_a$, -C*H*CH$_3$), 4.18 (bm, 76H$_e$, -OC*H*$_2$CH$_2$), 3.63 (bm, 304H$_{f,g,h,i}$, - C*H*$_2$OC*H*$_2$C*H*$_2$OC*H*$_2$), 3.54 (m, 76H$_j$, -C*H*$_2$OCH$_3$), 3.37 (m, 114H$_k$, -CH$_2$OC*H*$_3$), 2.32 (bs, 38H$_d$, -C*H*CH$_2$), 1.65 (m, 80H$_{c,l,m}$, -CHC*H*$_2$; -SC*H*$_2$C*H*$_2$; H$_2$O from CDCl$_3$), 1.25 (m, 2H$_j$, - C*H*$_2$CH$_3$); 1.15 (m, 3H$_b$, -CHC*H*$_3$), 0.93 (t, 3H$_m$, - CH$_2$C*H*$_3$)

m2P_n18: ^{1}H-NMR (400 MHz, CDCl$_3$): δ = ppm 8.38 (d, 1H$_a$, -NC*H*), 7.59 (m, 2H$_{b,c}$, -NCHC*H*C*H*), 7.01 (m, 1H$_d$, -NCC*H*), 4.74 (m, 1H$_g$, -C*H*CH$_3$), 4.10 (bm, 38H$_{f,k}$, -C*H*$_2$OCO; -OC*H*$_2$CH$_2$), 3.53 (bm, 72H$_{l,m}$, -OCH$_2$C*H*$_2$OC*H*$_2$), 3.43 (bm, 36H$_n$, -C*H*$_2$OCH$_3$), 3.27 (bs, 54H$_o$, -CH$_2$OC*H*$_3$), 2.94 (t, 2H$_e$, -SSC*H*$_2$), 2.26 (bs, 18H$_j$, -C*H*CH$_2$), 1.57 (m, 42H$_{i,p,q,r}$, -CHC*H*$_2$; -SCSC*H*$_2$C*H*$_2$C*H*$_2$CH$_3$), 1.05 (m, 3H$_h$, - CHC*H*$_3$), 0.83 (t, 3H$_s$, -CH$_2$C*H*$_3$)

m2P_n38: ^{1}H-NMR (400 MHz, CDCl$_3$): δ = ppm 8.47 (d, 1H$_a$,-NC*H*), 7.68 (m, 2H$_{b,c}$,-NCHC*H*C*H*),7.10 (m, 1H$_d$, -NCC*H*), 4.82 (m, 1H$_g$, -C*H*CH$_3$), 4.19 (bm, 76H$_k$, -C*H*CH$_3$), 3.62 (m, 152H$_{l,m}$, -OCH$_2$C*H*$_2$OC*H*$_2$), 3.52 (m, 76H$_n$, -C*H*$_2$OCH$_3$), 3.36 (bs, 114H$_o$, - C*H*$_2$OCH$_3$), 3.03 (m, 2H$_e$, -SSC*H*$_2$), 2.34 (bs, 38H$_j$, -C*H*CH$_2$), 1.66 (m, 82H$_{i,p,q,r}$, -CHC*H*$_2$; -SCSC*H*$_2$C*H*$_2$C*H*$_2$; H$_2$O from CDCl$_3$), 1.15 (m, 3H$_h$, -CHC*H*$_3$), 0.93 (t, 3H$_s$, -CH$_2$C*H*$_3$)

m2P_n50: ^{1}H-NMR (400 MHz, CDCl$_3$): δ = ppm 8.60 (d, 1H$_a$, -NC*H*), 7.93 (m, 2H$_{b,c}$, -NCHC*H*C*H*), 7.35 (m, 1H$_d$, -NCC*H*), 4.83 (m, 1H$_g$, -C*H*CH$_3$), 4.19 (bs, 102H$_{f,k}$, -C*H*$_2$OCO; -OC*H*$_2$CH$_2$), 3.65 (m, 202H$_{l,m,p}$ –OCH$_2$C*H*$_2$OC*H*$_2$; -SC*H*$_2$), 3.52 (m, 100H$_n$, -C*H*$_2$OCH$_3$), 3.36 (s, 150H$_o$, -CH$_2$OC*H*$_3$), 3.12 (m, 2H$_e$, -SSC*H*$_2$), 2.33 (bs, 50H$_j$, -C*H*CH$_2$), 1.65 (m, 104H$_{i,q,r}$, -CHC*H*$_2$; -SCSCH$_2$C*H*$_2$; -C*H*$_2$CH$_3$; H$_2$O from CDCl$_3$), 1.15 (m, 3H$_h$, - CHC*H*$_3$), 0.93 (t, 3H$_s$, -CH$_2$C*H*$_3$)

m1C_n53: ^{1}H-NMR (400 MHz, CDCl$_3$): δ = ppm 4.84 (m, 1H$_a$, -C*H*CH$_3$), 4.19 (bm, 106H$_e$,-OC*H*$_2$CH$_2$), 3.56 (m, 106H$_f$, -C*H*$_2$OCH$_3$), 3.35 (bs, 159H$_g$, -CH$_2$OC*H*$_3$), 2.39 (bs, 53H$_d$, -C*H*CH$_2$), 1.68 (m, 112H$_{c,h,i,j}$, -CHC*H*$_2$; -SC*H*$_2$C*H*$_2$C*H*$_2$), 1.17 (m, 3H$_b$, -CHC*H*$_3$), 0.92 (t, 3H$_k$, - CH$_2$C*H*$_3$)

m9C_n14: ^{1}H-NMR (400 MHz, CDCl$_3$): δ = ppm 4.82 (m, 1H$_a$, -C*H*CH$_3$), 4.17 (bs, 28H$_e$, -OC*H*$_2$CH$_2$), 3.63 (bm, 476H$_{f,g,h,i}$, -C*H*$_2$OC*H*$_2$C*H*$_2$OC*H*$_2$), 3.55 (m, 28H$_j$, -C*H*$_2$OCH$_3$), 3.36 (m, 42H$_k$, -CH$_2$OC*H*$_3$), 2.32 (bs, 14H$_d$, -C*H*CH$_2$), 1.66 (m, 64H$_{c,l,m,n}$, -CHC*H*$_2$; -SC*H*$_2$C*H*$_2$C*H*$_2$; H$_2$O from CDCl$_3$), 1.13 (m, 3H$_b$, - CHC*H*$_3$), 0.93 (t, 3H$_o$, -CH$_2$C*H*$_3$)

m9C_n30: ^{1}H-NMR (400 MHz, CDCl$_3$): δ = ppm 4.80 (m, 1H$_a$, -C*H*CH$_3$), 4.16 (bs, 62H$_{e,l}$, -OC*H*$_2$CH$_2$; SCSC*H*$_2$), 3.63 (bm, 960H$_{f,g,h,i}$, -C*H*$_2$OC*H*$_2$C*H*$_2$OC*H*$_2$), 3.54 (m, 60H$_j$, -C*H*$_2$OCH$_3$), 3.37 (m, 90H$_k$, -CH$_2$OC*H*$_3$), 2.30 (bs, 30H$_d$, -C*H*CH$_2$), 1.67 (m, 64H$_{c,m,n}$, -CHC*H*$_2$; -SC*H*$_2$C*H*$_2$; H$_2$O from CDCl$_3$), 1.13 (m, 3H$_b$, -CHC*H*$_3$), 0.93 (t, 3H$_o$, -CH$_2$C*H*$_3$)

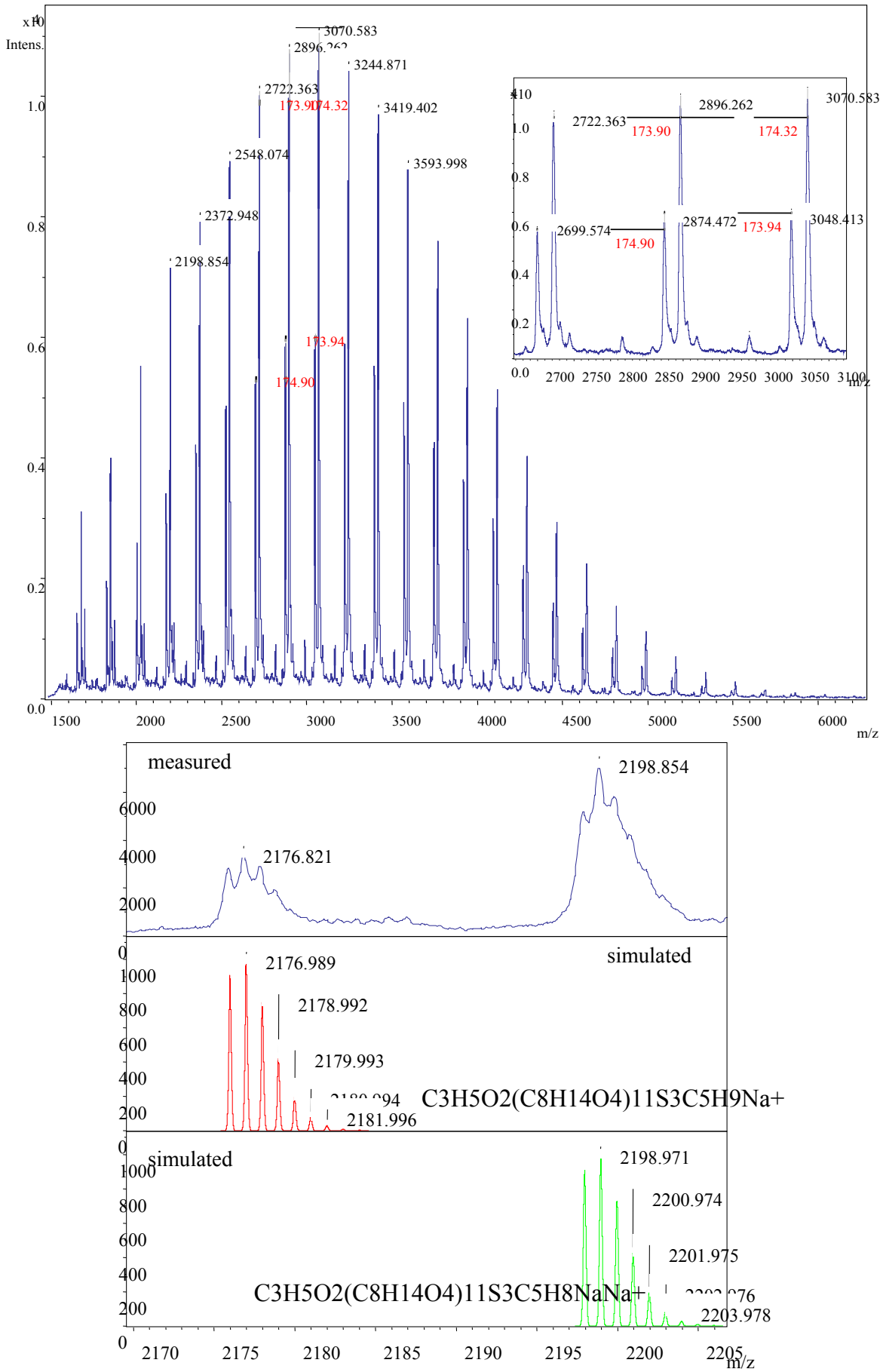

Figure S12. MALDI-TOF spectrum of poly(methoxy di(ethylene glycol)acrylate) (**m2C_n16**).

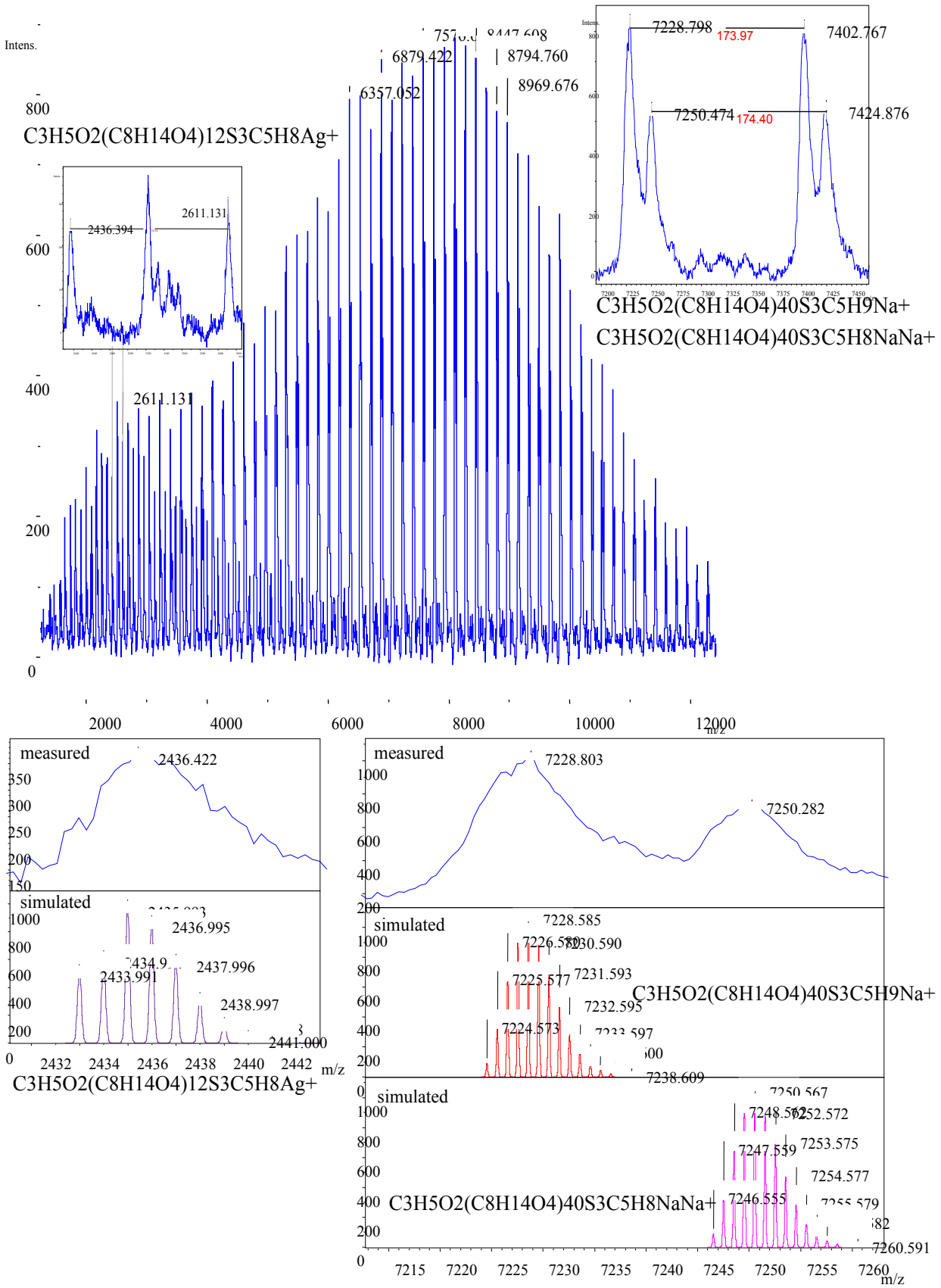

Figure S13. MALDI-TOF spectrum of poly(methoxy di(ethylene glycol)acrylate) (**m2C_n49**).

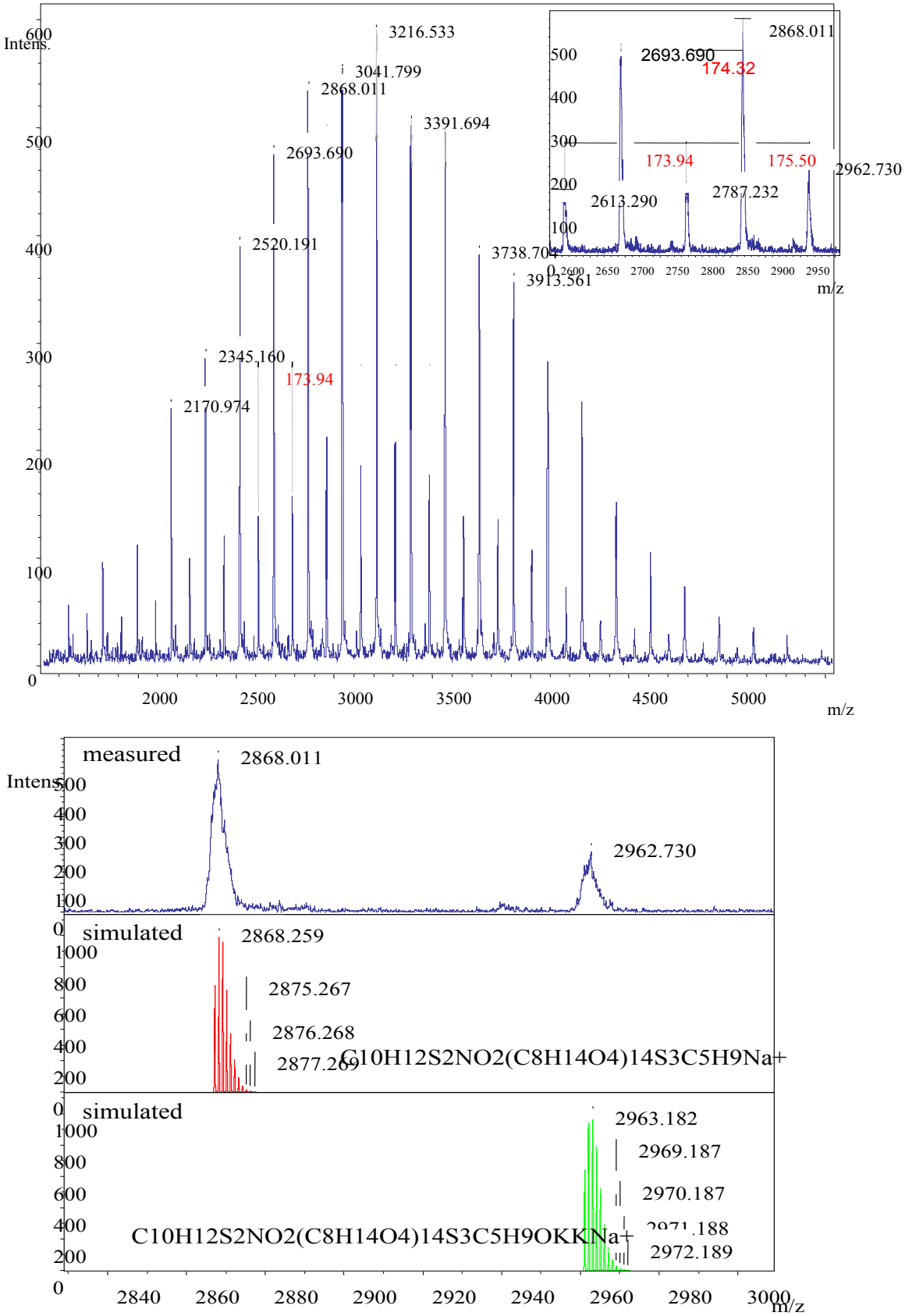

Figure S14. MALDI-TOF spectrum of poly(methoxy di(ethylene glycol)acrylate) (**m2P_n18**).

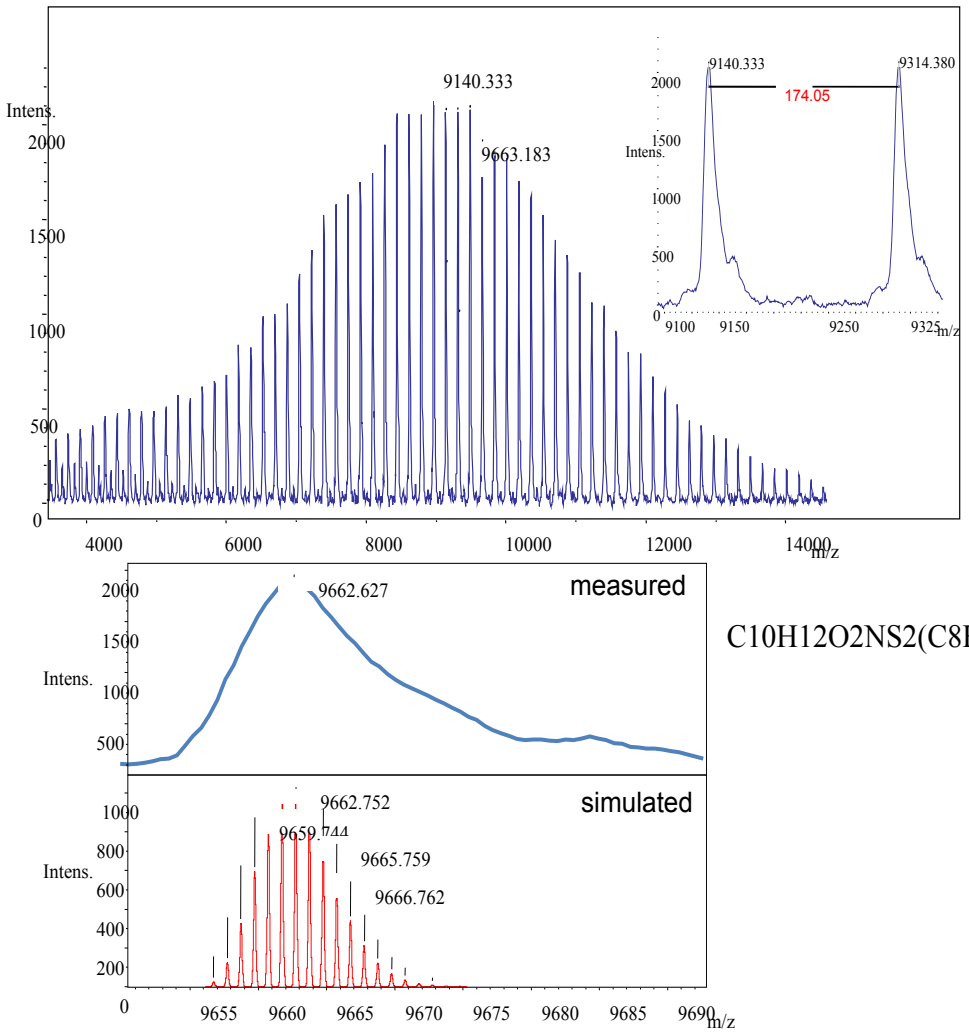

Figure S15. MALDI-TOF spectrum of poly(methoxy di(ethylene glycol)acrylate) (**m2P_n50**).

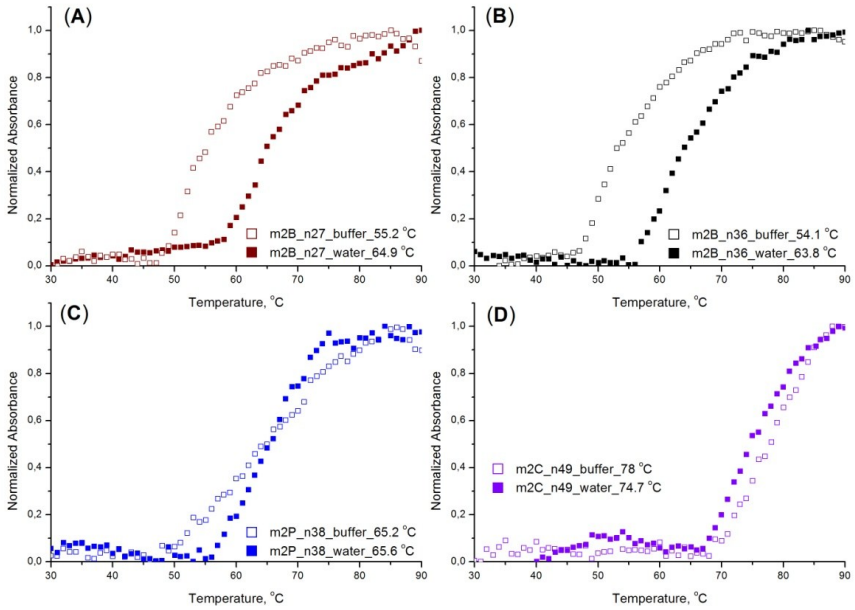

Figure S16. LCST (T_{cp}) measurements for the polymers **(A) m2B_n27, (B) m2B_n36, (C) m2P_n38, (D) m2C_n49** either as 10 μM solution in a 50 mM Na_2HPO_4 buffer (pH 7.4) supplemented with 150 mM NaCl or as 10 μM solution in water.

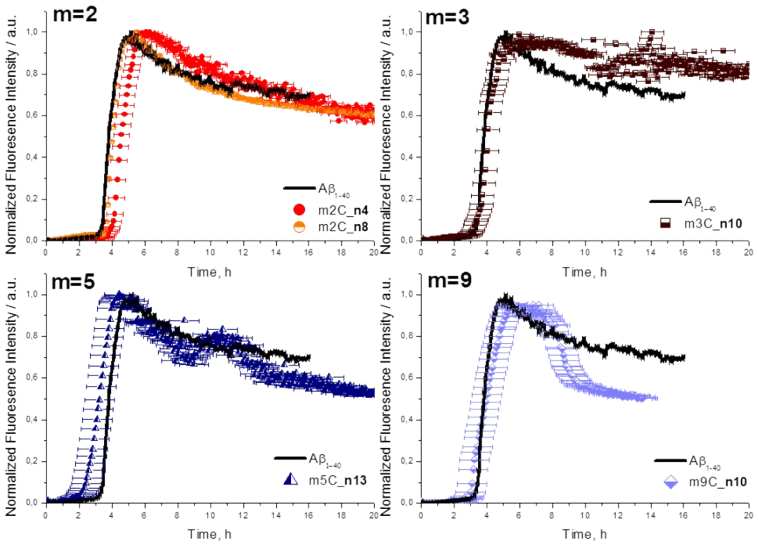

Figure S17. Time evolution of the ThT fluorescence intensity of the poly(oligo(ethylene glycol)$_m$ acrylates) / A$\beta_{1\text{-}40}$ mixtures at λ = 480 nm. Black solid line corresponds to A$\beta_{1\text{-}40}$ wild type. The hydrophilicity is varied by the number of ethylene glycol units (m). Degree of polymerization (n) is indicated for every sample and highlighted in bold. Error bars based on three independent measurements are shown.

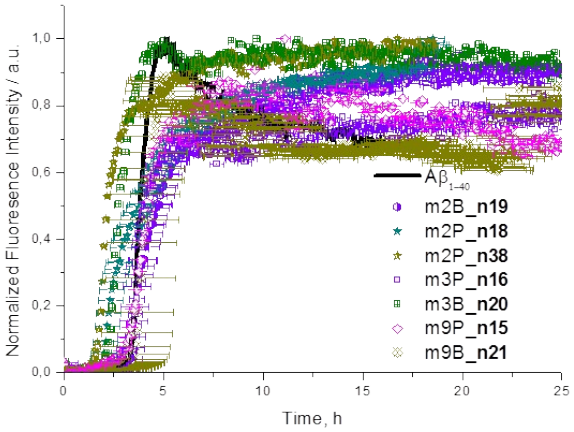

Figure S18. Effect of the polymer's end-group on the t_{lag} and t_{char} of the A$\beta_{1\text{-}40}$ fibrillation demonstrated as a time evolution of the ThT fluorescence intensity at λ = 480 nm. Error bars based on three independent measurements are shown.

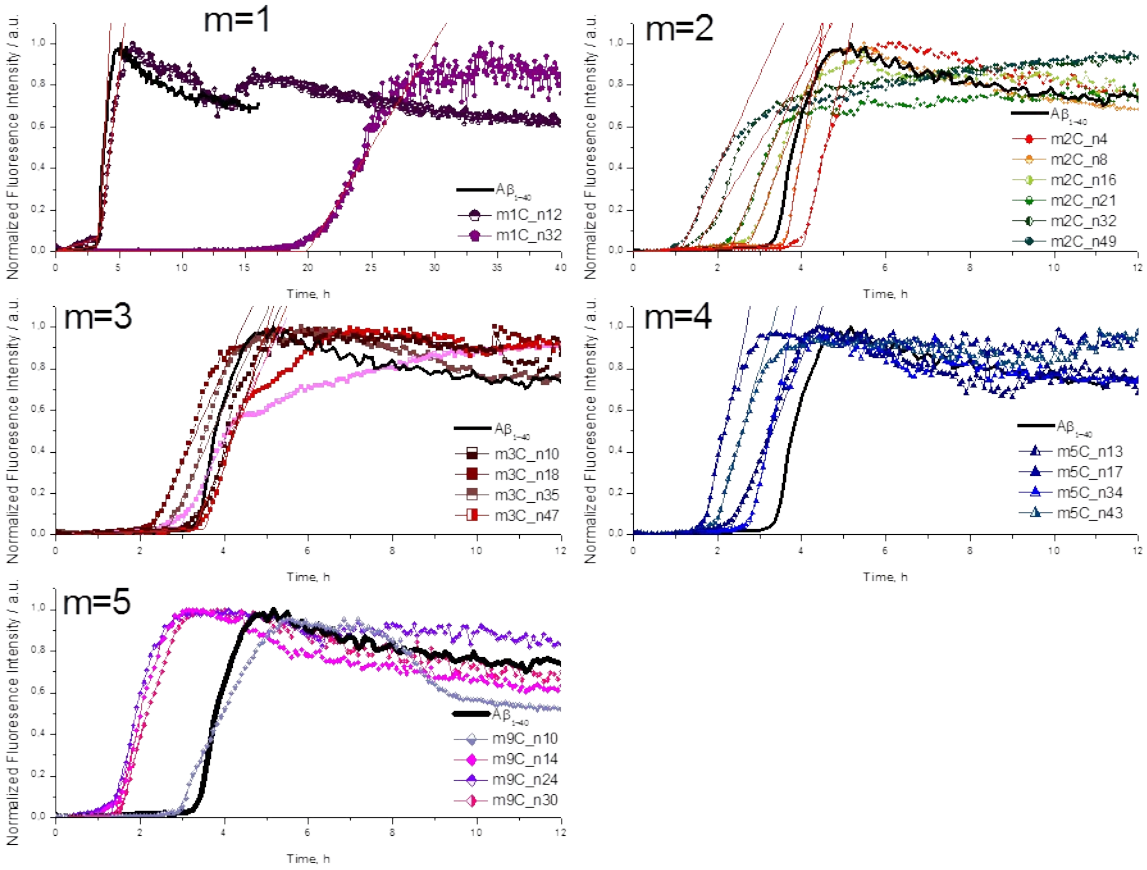

Figure S19. Time evolution of the ThT fluorescence intensity of the poly(oligo(ethylene glycol)m acrylates) / Aβ1-40 mixtures at λ = 480 nm. Black solid line corresponds to Aβ1-40 wild type. The hydrophilicity is varied by the number of ethylene glycol units (m). Degree of polymerization (n) is indicated for every sample and highlighted in bold. Piecewise linear fits are demonstrated respectively.

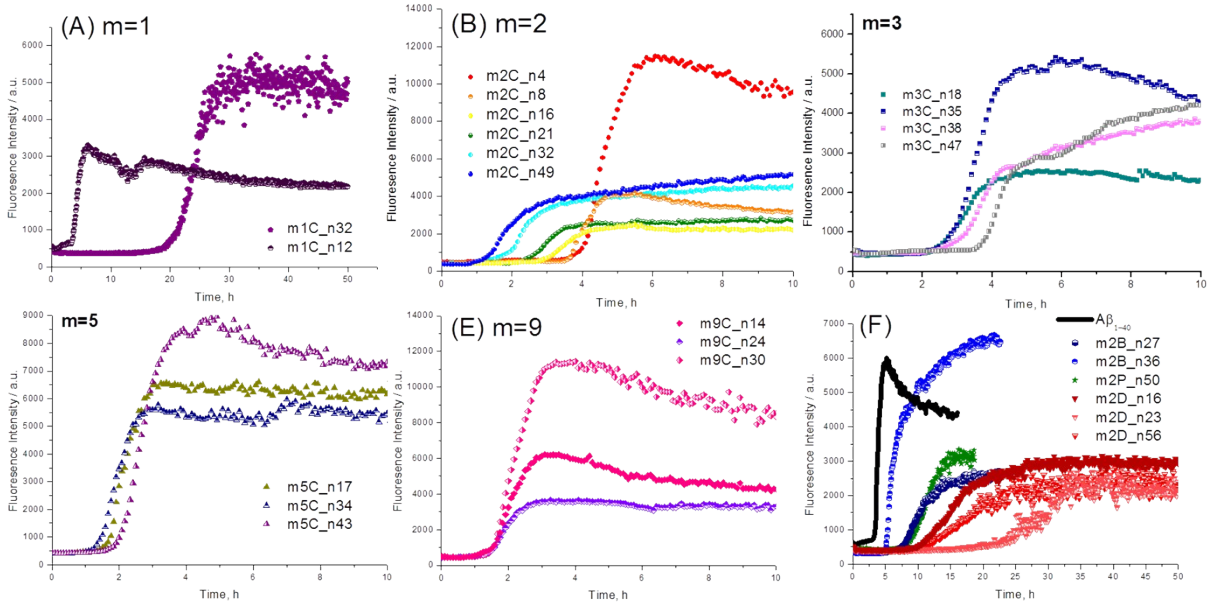

Figure S20. Time evolution of the ThT fluorescence intensity of the poly(oligo(ethylene glycol)$_m$ acrylates) / A$\beta_{1\text{-}40}$ mixtures at λ = 480 nm. Black solid line corresponds to A$\beta_{1\text{-}40}$ wild type. The raw data are presented. The hydrophilicity is varied by the number of ethylene glycol units (m=1-9) ((A)-(E)) and by choice of the end groups (F).

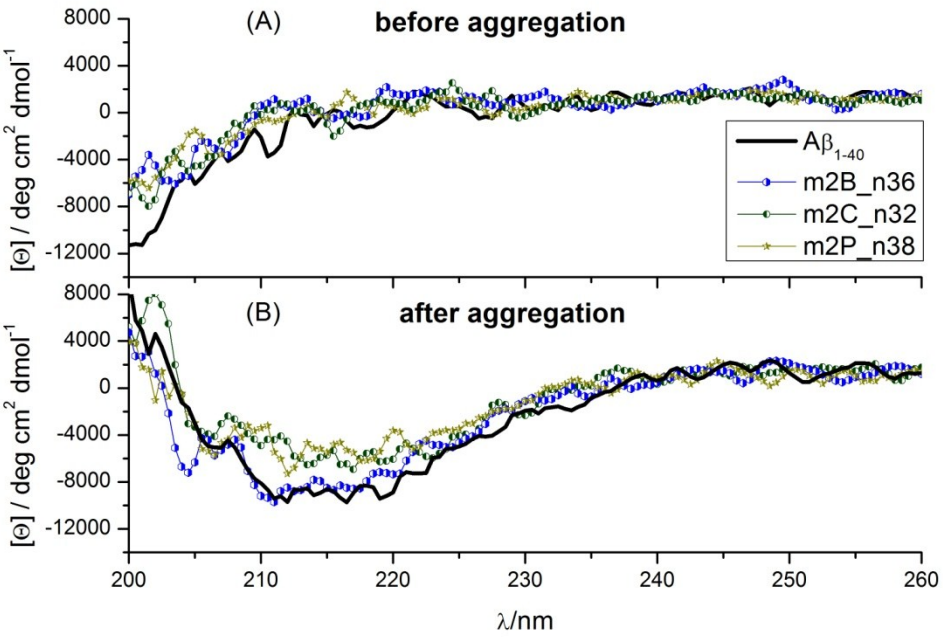

Figure S21. UV-CD spectra of the Aβ$_{1-40}$ / poly(oligo(ethylene glycol)$_m$ acrylates) **m2B_n36**, **m2C_n32**, **m2P_n38** 10 μM/10 μM mixtures as solution in a 50 mM Na_2HPO_4 buffer (pH 7.4) supplemented with 150 mM NaCl, measured (**A**) just before ThT kinetic measurements and (**B**) just after ThT kinetic measurements. The resulting CD spectra display a transition from the non-aggregated freshly prepared native peptides (**A**) to the β-sheet rich fibrils (**B**).

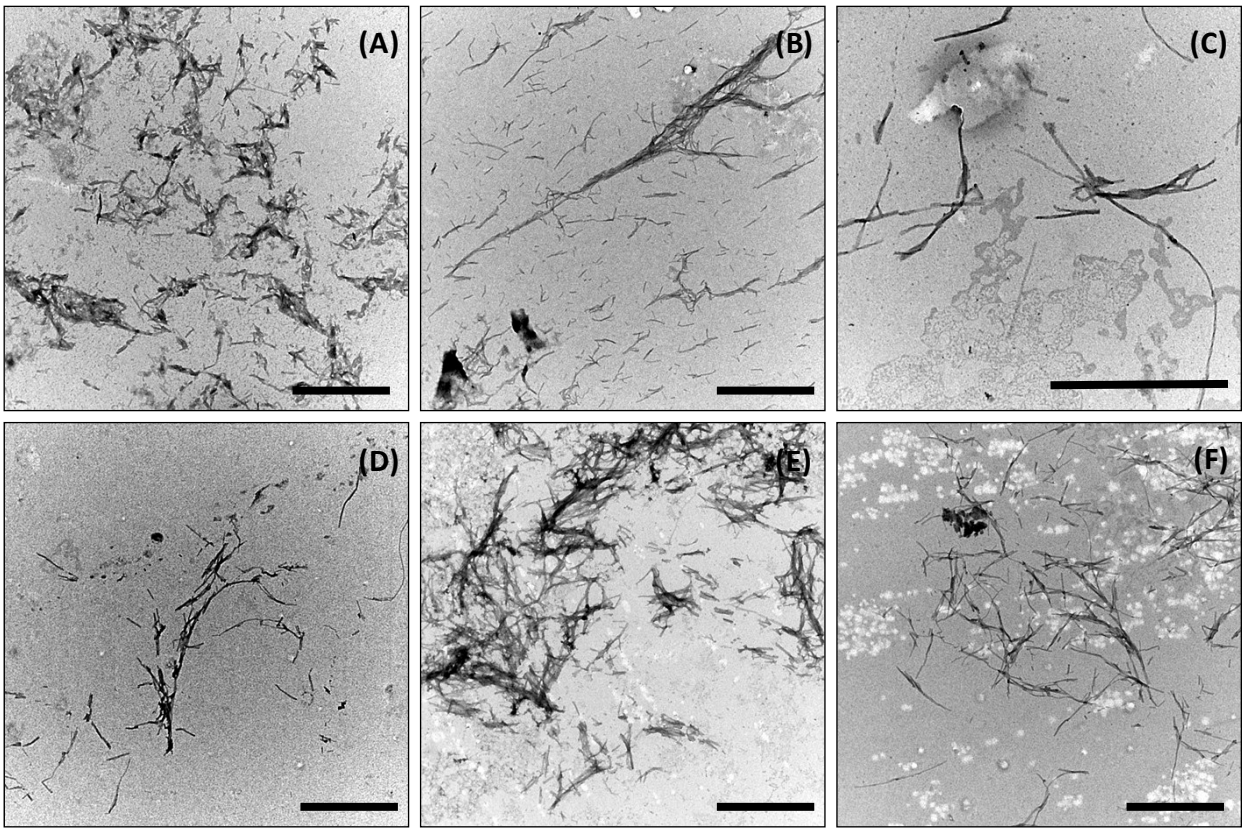

Figure S22. TEM images of the fibrils obtained after ThT kinetic measurements (A) Aβ$_{1-40}$ / m2P_n38 ; (B) Aβ$_{1-40}$ / m1C_n32; (C) Aβ$_{1-40}$ / m2D_n16; (D) Aβ$_{1-40}$ / m3C_n10; (E) Aβ$_{1-40}$ / m5C_n13; (F) Aβ$_{1-40}$ / m9C_n10. The scale bar corresponds to 1000 nm.

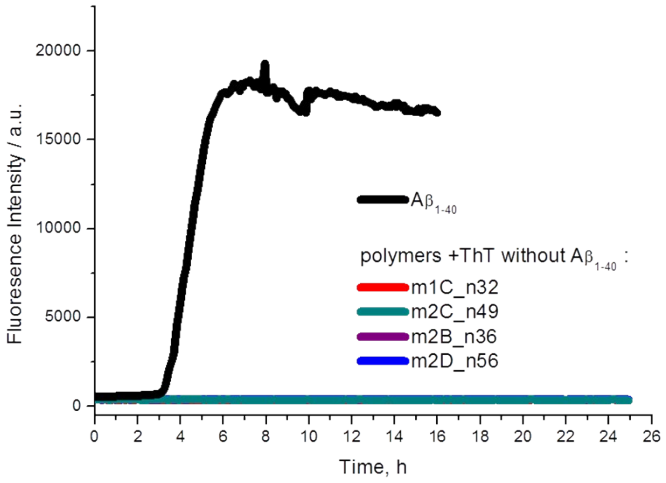

Figure S23. Time evolution of the ThT fluorescence intensity of the poly(oligo(ethylene glycol)$_m$ acrylates) m1C_n32, m2C_n49, m2B_n36 and m2D_n56 at λ = 480 nm. Black solid line corresponds to A$\beta_{1\text{-}40}$ wild type.

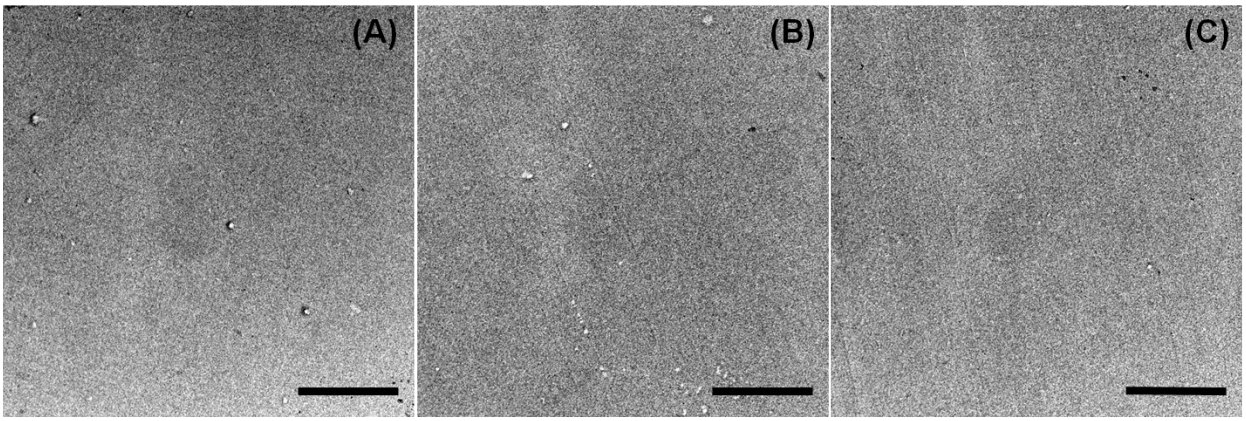

Figure S24. TEM images of the polymers (A) m1C_n32, (B) m2D_n56 and (C) m2C_n49 obtained after ThT kinetics studies.

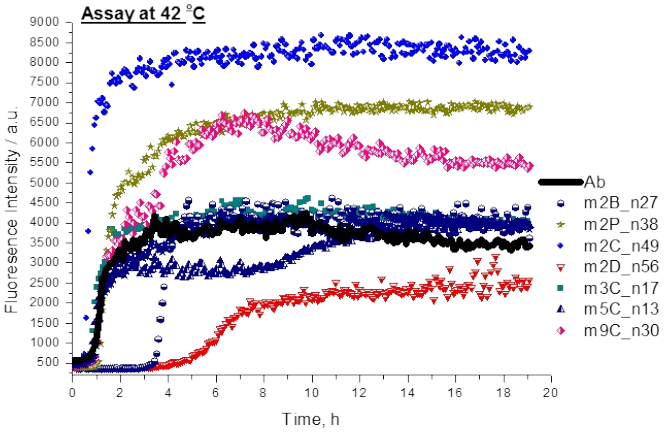

Figure S25 Time evolution of the ThT fluorescence intensity of the poly(oligo(ethylene glycol)$_m$ acrylates) / A$\beta_{1\text{-}40}$ mixtures at λ = 480 nm and 42 °C. Black solid line corresponds to A$\beta_{1\text{-}40}$ wild type. The raw data are presented.

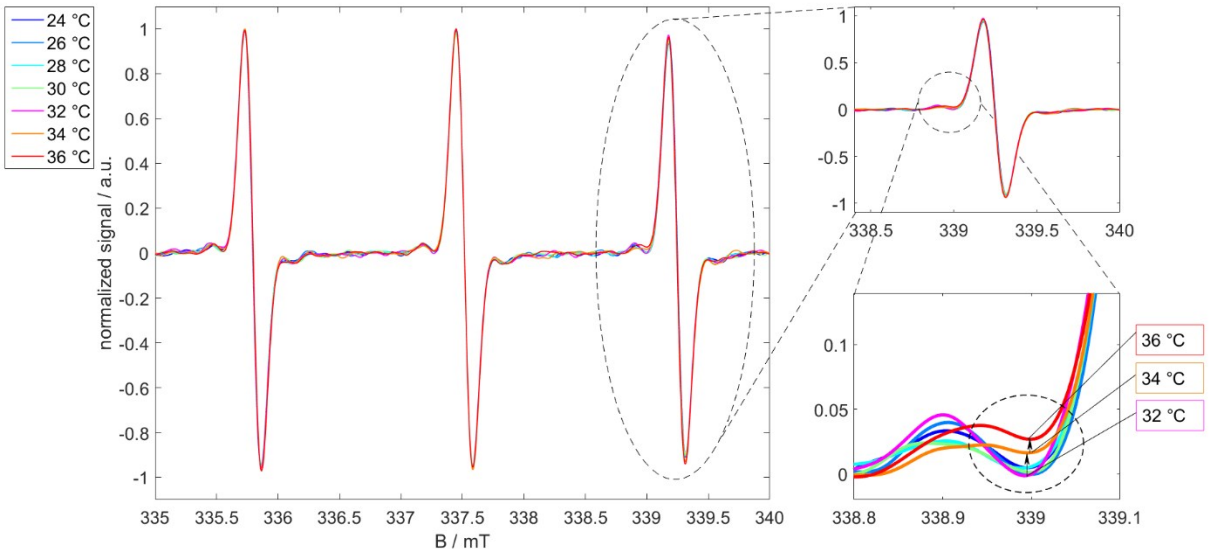

Figure S26 CW EPR spectra of the physical mixture of polymer (15) m2D_n23 and $A\beta_{1\text{-}40}$ at different temperatures. Starting at temperatures of 34°C, a second type of spectral component becomes visible in particular at the high-field EPR line (see inset and zoom), which clearly stems from TEMPO probe molecules that on the timescale of our EPR experiment (nanoseconds) reside in water-depleted, polymer-enriched "hydrophobic" nano-inhomogeneities.

(1) Scarano, W.; Duong, H. T. T.; Lu, H.; De Souza, P. L.; Stenzel, M. H. *Biomacromolecules* **2013**, *14*, 962-975.

(2) Ferguson, C. J.; Hughes, R. J.; Nguyen, D.; Pham, B. T. T.; Gilbert, R. G.; Serelis, A. K.; Such, C. H.; Hawkett, B. S. *Macromolecules* **2005**, *38*, 2191-2204.